AUTHOR QUERY FORM

ELSEVIER	**Journal:** IJLEO **Article Number:** 52329	**Please e-mail or fax your responses and any corrections to:** **E-mail:** corrections.esch@elsevier.thomsondigital.com **Fax:** +353 6170 9272

Dear Author,

Please check your proof carefully and mark all corrections at the appropriate place in the proof (e.g., by using on-screen annotation in the PDF file) or compile them in a separate list. Note: if you opt to annotate the file with software other than Adobe Reader then please also highlight the appropriate place in the PDF file. To ensure fast publication of your paper please return your corrections within 48 hours.

For correction or revision of any artwork, please consult http://www.elsevier.com/artworkinstructions.

Any queries or remarks that have arisen during the processing of your manuscript are listed below and highlighted by flags in the proof. Click on the 'Q' link to go to the location in the proof.

Location in article	Query / Remark: click on the Q link to go Please insert your reply or correction at the corresponding line in the proof
Q1	Please confirm that given names and surnames have been identified correctly.
Q2	Please check that the affiliations link the author 'E.M. Sheha' with their correct departments, institutions, and locations, and correct if necessary.
Q3	Please check the affiliation, and correct if necessary.
Q4	Please check the address for the corresponding author that has been added here, and correct if necessary.
Q5	Please provide the keywords.
Q6	Please check the edit made in the sentence "Conducting . . . so on", and correct if necessary.
Q7	Please check the edit made in the sentence "The crucial . . . material", and correct if necessary.
Q8	Please check the edit made in the sentence "In the present . . . spectra", and correct if necessary.
Q9	To maintain sequential order, Eq. (3) has been changed to Eq. (2); Eq. (4) to Eq. (3); Eq. (5) to Eq. (4); Eq. (2) to Eq. (5). Please check, and correct if necessary.
Q10	Please check the edit made in the sentence "The direct . . . Table 1", and correct if necessary.
Q11	Please check the edit made in the sentence "The values . . . Table 2", and correct if necessary.
Q12	The citation of Table 3 has been changed to Table 2; Table 2 to Table 3 to match with tables. Please check, and correct if necessary.
Q13	Please check the edit made in the sentence "where Eb . . . respectively", and correct if necessary.
Q14	Please check the edit made in the sentence "The hole . . . composite", and correct if necessary.
Q15	Please provide the complete details for Ref. [7].
Q16	Please check the author names for Ref. [14].
Q17	Please check the page number for Ref. [26].
	Please check this box if you have no corrections to make to the PDF file ☐

Location in article	Query / Remark: click on the Q link to go Please insert your reply or correction at the corresponding line in the proof

Thank you for your assistance.

Optik xxx (2012) xxx–xxx

Contents lists available at SciVerse ScienceDirect

Optik

journal homepage: www.elsevier.de/ijleo

Characterization of PVA/CuI polymer composites as electron donor for photovoltaic application

Q2 M.K. El-Mansy[a,*], E.M. Sheha[a,b,c], K.R. Patel[b], G.D. Sharma[b,c,**]

[a] Department of Physics, Faculty of Science, Benha University, Benha, Egypt
Q3 [b] Molecular Electronic and Optoelectronic Device Laboratory, Physics Department, JNV University, Jodhpur (Raj.) 342005, India
[c] R & D Centre for Science and Technology, JEC Group of Colleges, Kukas, Jaipur (Raj.), India

ARTICLE INFO

Article history:
Received 19 December 2011
Accepted 2 May 2012

ABSTRACT

Q5 Nanopolymer composite of PVA/CuI has been prepared as in both colloidal forms and solid layers and characterized their structure by X-ray diffraction, scanning electron microscopy, AC spectroscopy and optical absorption in UV–visible. It is observed that with the growth of CuI nanoparticles (in the range of 26–46 nm in size) reduces the PVA polymer crystallinity. The temperature dependence of bulk conductivity for PVA/CuI nanocomposite illustrated that the composites behave as the semiconducting materials with the activation energy in the range of 0.27–1.02 eV. It was observed that the direct optical band gap reduces from 3.53 eV to 1.7 eV as the concentration of CuI nanoparticles in the PVA increased from 0% to 10%. The highest occupied molecular orbital (HOMO) and lowest unoccupied molecular orbital (LUMO) energy levels of the PVA/CuI nanocomposites were estimated from the cyclic voltammetry. The electrochemical band gap, that is, the difference between HOMO and LUMO levels also decreases with the increase in the concentration of the CuI in PVA, which is in agreement with the trend observed in the optical band gap. The current–voltage characteristics of the devices based on PVA/CuI nanocomposites, in dark shows that these composites behave as p-type semiconductors. We have also investigated the *J–V* characteristics under illumination and found that the power conversion efficiency is very low but these composites can be used as electron donor for bulk heterojunction solar cells along with fullerene derivatives as electron acceptor.

1. Introduction

Solar energy conversion devices based on organic semiconductors are an emerging research field with substantial future prospects and it has attracted great attention due to the advantages of light weight, flexibility and low cost of production with the possibility of fabricating large area devices based on solution processing. Achieving efficient solar energy conversion on a large scale and at low cost is one of the most important challenges for the near future. New materials and fabrication procedures leading to the substantial reduced cost of photovoltaic electricity could help drive a rapid expansion in the implementation of photovoltaic technology .The need to improve the light-to-electricity conversion efficiency requires the implementation of such materials and the exploration of new device architectures [1–8]. During last two years, synthesis and design of several important low band gap polymers with enhanced absorption abilities have been reported and researchers made a breakthrough in fabricating polymer solar cells with power conversion efficiency (PCE) up to 5–7% based on the BHJ active layer using these polymers as electron donor along with the fullerene derivatives as electron acceptor [9]. To date, the PCEs based on conjugated polymer solar cells have reached a high up to 8.13% by Solarmer [10a] and 8.3% by Konarka [10b].

It is well known that the electrical and optical properties of polymers can be improved to a desired limit through suitable doping [11]. Further, polymers, on doping with metal nanoparticles, show novel and distinctive properties obtained from the unique combination of the inherent characteristics of polymers and properties of the metal nanoparticles [12]. The optical and electrical properties of nanocomposites films can be adjusted by varying the composition.

Over the years, polyvinyl alcohol (PVA) polymers have attracted attention due to their variety of applications. PVA is a potential material having high dielectric strength, good charge storage capacity and dopant-dependent electrical and optical properties. It has carbon chain backbone with hydroxyl groups attached to methane carbons; these OH groups can be a source of hydrogen bonding and hence assist the formation of polymer composite [13].

* Corresponding author.
Q4 ** Corresponding author at: Molecular Electronic and Optoelectronic Device Laboratory, Physics Department, JNV University, Jodhpur (Raj.) 342005, India.
E-mail addresses: elmansyymabrouk@yahoo.com, Mabrouk.almansy@fsc.bu.edu.eg (M.K. El-Mansy).

0030-4026/$ – see front matter © 2012 Published by Elsevier GmbH.
http://dx.doi.org/10.1016/j.ijleo.2012.05.009

Cuprous iodide (CuI) has attracted a great attention, as it is a versatile candidate in band gap materials (CuI, CuSCN, and $CuAlO_2$) that were identified in the preparation of optical properties of thin film. CuI belongs to the I–VII semiconductors with zinc blend structure. Conducting materials and optically transparent films aroused much interest in the capability of application in electronic devices such as liquid crystal displays, photovoltaic devices, photothermal collectors and so on. The most interesting nature of this compound is that an inorganic semiconductor and its coordination chemistry let it readily couple with many inorganic and organic ligands as well [13–18].

The optical and electrical properties of semiconductor nanoparticles depend mainly on their shape and size due to high surface-to-volume ratio [19,20]. The use of polymers is a prominent method for the synthesis of semiconductor nanoparticles. The reason is that the polymer matrices provide for processability, solubility, and control of the growth and morphology of the nanoparticles.

The crucial factors for the use of a semiconducting material as an active layer in the solar cells are the band gap and optical absorption of the material. The relatively large band gap of polymer such as PVA limits the absorption of near-infrared light and thus lowers the light harvesting and therefore cannot be used as an active layer in organic solar cells. The control over the band gap is necessary while designing new materials for organic solar cells. The band gap engineering allows one to design and synthesize new materials with maximum overlap of absorption spectrum with the solar emission spectrum. It is often found that the synthesis of low band gap polymer is not only the solution to address this problem but also the position of highest occupied molecular orbital (HOMO) and lowest unoccupied molecular orbital (LUMO) limits the open-circuit voltage (V_{oc}) of the photovoltaic cell. These two properties of organic materials can be controlled by introducing nanoinorganic salts or introducing alternative electron rich and electron-deficient units in the polymer backbone [6,7].

In the present work, we prepared and characterized the PVA polymer with and without the inorganic salt CuI nanoparticles to produce p-type PVA/CuI nanocomposite with suitable energy band gap which matches with the solar energy spectra. We applied these nanocomposite layers to fabricate the device having ITO/PEDOT:PSS/CuI–PVA/Al and found that these nanoparticles behave as p type semiconducting materials forming the Schotky barrier for electron injection PVA–CuI/Al interface, whereas the ITO/PEDOT:PSS electrode forms the Ohmic contact in the device. The power conversion efficiency (PCE) of these devices is very low but can be used as electron donor for BHJ photovoltaic device along with fullerene derivatives to improve the PCE; this work is under progress.

2. Experimental

A polyvinyl alcohol polymer (PVA) used in the present study was purchased from by Sigma–Aldrich and the other chemicals were provided by QualiKems Chemical Company, India. A PVA solution was prepared by adding deionized distilled water to solid PVA ($-C_2H_4O)_n$ (where n = 30,000–70,000, average molecular weight) and then stirred by a magnetic stirrer at room temperature, 30 °C, for 2 h. After aging the solution for another 1 h, a solution of $CuCl_2$ in H_2O was added into the PVA solution under constant stirring and then the appropriate weight of NaI dissolved in water was added 2 h dropwise into the reaction vessel to obtain nanopolymer composite with different concentrations of CuI (0–15 wt%), followed by stirring for another 2 h. The as prepared polymer composite was directly cast in a Petri-glass dishes and left for two weeks at room temperature 30 °C to dry. These CuI–PVA nanocomposites are easily soluble in DMF and DMSO solvents.

In order to investigate the structure of the polymer electrolyte layers, X-ray diffraction studies were carried out using ShIMADZU diffractometer type XRD 6000, wave length λ = 1.5418 Å. In addition, the surface morphology of these nanocomposites was also examined using scanning electron microscope, SEM (JOEL-JSM Model 5600).

The CuI–PVA thick films of thickness of about 0.4 mm were used to measure the bulk conductivity measurements. The silver paste was used as conducting electrodes on both sides of the film. Electrical measurements were carried out in the temperature range 303–373 K using PM 6304 programmable automatic RCL Philips meter in the frequency range 0.1–100 kHz. The optical absorption of both colloidal and solid films of CuI–PVA was measured in the wavelength range 190–1100 nm using JENWAY 6405 UV–visible spectrophotometer at room temperature.

The electrochemical cyclic voltammetry was conducted on the electrochemical instrument in a 0.1 mol L acetornitrile solution of tetrabutylammonium hexafluorophosphate (Bu_4NPF_6) at a potential scan rate of 100 mV/s using Ag/AgCl reference and platinum wire as counter electrodes, respectively. The composite film was formed by drop casting of composite solution in DMF on the working electrode.

The ITO/PEDOT:PSS/CuI–PVA composites/Al devices were fabricated on the pre-cleaned indium tin oxide coated (ITO) coated glass substrates. A layer of PEDOT:PSS (80 nm) was deposited on ITO coated glass substrate from poly (3,4-ethylenedioxythiophene):poly (styrensulfonate) (PEDOT:PSS) aqueous solution at 2000 rpm and the layer was subsequently dried at 100 °C for 20 min in air. The CuI–PVA nanocomposites in different concentrations (10 mg/mL) were dissolved in DMF solvent under constant stirring for 2 h and the spin coated (2000 rpm for 20 s) on the top of the PEDOT:PSS layer and then dried under ambient condition. The device was completed with depositing of 90 nm thick layer of aluminum (Al) at a pressure of less than 10^{-5} Torr.

The current–voltage characteristics (J–V) of the devices were measured on a computer controlled Keithley electrometer in dark and under illumination of the intensity (100 mW/cm^2), at room temperature. A xenon lamp was used as a light source to give the stimulated irradiance of 100 mW/cm^2 at the surface of the device. To measure the charge carrier mobility, the device having structure ITO/PEDOT:PSS/CuI–PVA composite/Au was fabricated as described above except the top electrode was replaced by Au. The J–V characteristics of these devices were measured as described earlier, in dark.

3. Results and discussions

3.1. PVA polymer nanocomposite characterizations

The XRD patterns of the as-prepared CuI-polymer composites are shown in Fig. 1. As can be seen from these XRD patterns that a broad peak appeared around 2θ = 19.12° which is the characteristic peak for PVA. As the CuI concentration was increased, new sharp peaks at 2θ = 25.49°, 42.24° and 49.99° were appeared, indicating the growth of CuI crystallite nanoparticles in the polymer matrix. A broadened peak with reduced intensity corresponding to PVA was observed and another sharp peak refers to the separation of NaCl crystallites in the polymer matrix was also detected. Our results are in agreement as report by Hodge et al. [21]. The three diffraction peaks for CuI as mentioned above correspond to the (0 1 2), (1 1 0) and (2 0 2) planes of CuI nanocrystals which could be indexed to hexagonal structure (the lattice constants are: a = 4.291 Å and

Please cite this article in press as: M.K. El-Mansy, et al., Characterization of PVA/CuI polymer composites as electron donor for photovoltaic application, Optik - Int. J. Light Electron Opt. (2012), http://dx.doi.org/10.1016/j.ijleo.2012.05.009

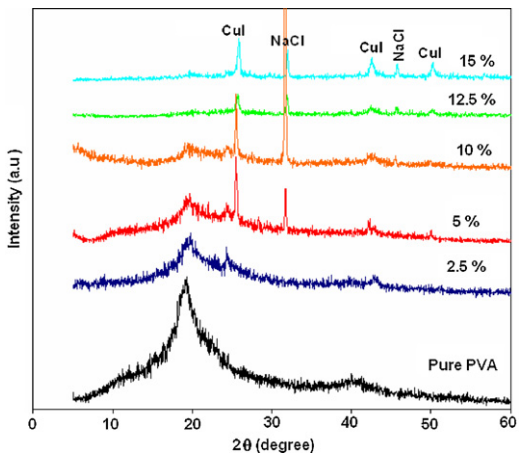

Fig. 1. XRD patterns for CuI/PVA composites with different concentration of CuI.

$c = 21.48$ Å), which were consistent with the literature data of JCPDS 83-1145. The average particle size can be calculated using the first sphere approximation of Debye–Scherrer formula [22]

$$D = \frac{0.9\lambda}{B\cos\theta} \quad (1)$$

where D is the average diameter of the crystals, λ is the wavelength of X-ray radiation, and B is the full width at half maximum intensity of the peak. The obtained particle size of CuI embedded in polymer composite obtained for different concentrations (0–15 wt%) of CuI lies in the range 25.6 and 46.7 nm (Table 1). The apparent fluctuation of the particle size of CuI phase may be attributed to the nanoparticles aggregation in the samples rich with CuI nanoparticles.

Scanning electron microscopy is also used to study the compatibility between various components of the CuI-polymer through the detection of phase separations and interfaces. Depending on the type and amount of salt present in the polymer matrix, the morphology of the CuI-polymer composite will vary and greatly influence its properties. Morphological examination was also carried out to demonstrate the phase changes of the pure polymer and the resulting solid PVA–CuI composite layers. Scanning electron micrographs of pure PVA, and some polymer-CuI nanocomposites are given in Fig. 2. Very distinguishable changes have been observed from pure PVA, to low, intermediate and high concentrations of CuI salt. Pure PVA shows smooth surface of the PVA film. The morphology changes, as 2.5 wt% of CuI salt is incorporated into the polymer, surface roughness became observable and nanostructure refers to the growth of nano-CuI particles. When a higher concentration of CuI nanoparticles was increased in polymer matrix to 10 wt%, the morphology changes drastically to become significantly more layered and even greater pore size besides the increase of surface roughness. An open pore structure of the polymer electrolyte matrix is essential for ionic conductivity across the thin film. This type of open porous structure provides enough channels ions migration, accounting for better ionic conductivity as well as the increase of surface area.

3.2. Optical absorption

The optical absorption spectrum is an important tool to obtain optical energy band gap of crystalline and amorphous materials. The fundamental absorption, which corresponds to the electron excitation from the valance band to the conduction band, can be used to determine the nature and value of the optical band gap. Fig. 3a and b illustrates the plot of the optical absorption against wavelength in the UV–visible range for polymer/CuI composites

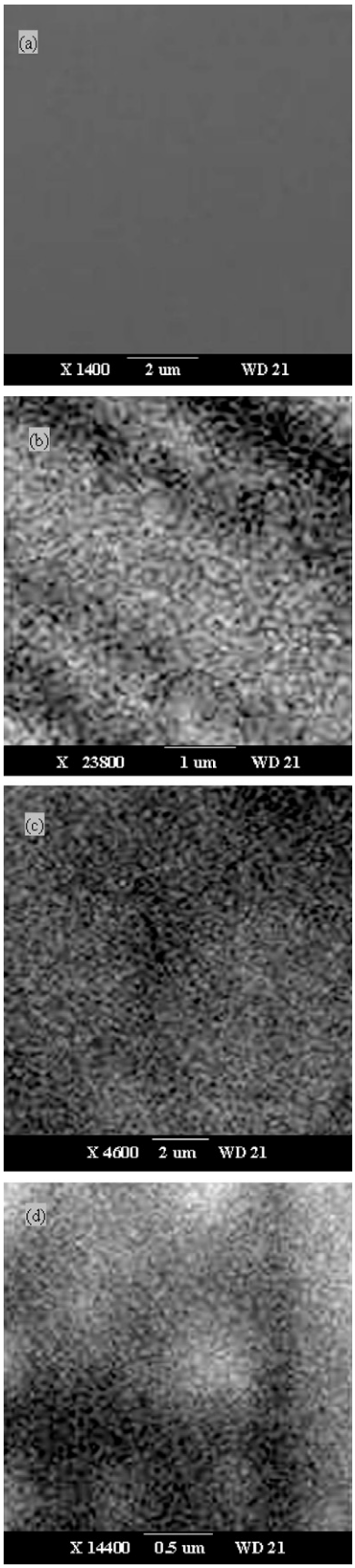

Fig. 2. SEM images for CuI/PVA nanocomposites with selected concentrations of CuI (a) pure PVA, (b) 2.5 wt%, (c) 5 wt% and (d) 10 wt%.

Please cite this article in press as: M.K. El-Mansy, et al., Characterization of PVA/CuI polymer composites as electron donor for photovoltaic application, Optik - Int. J. Light Electron Opt. (2012), http://dx.doi.org/10.1016/j.ijleo.2012.05.009

Table 1
Extracted optical energy gap (direct and indirect) for colloidal and solid films of PVA/CuI composites, Urbach energy, absorption peak position for colloidal composites.

CuI conc. (wt%)	Colloidal			Solid films			λ_{max} (nm) Colloidal
	E_{gd} (eV) (direct)	E_{gi} (eV) (indirect)	E_u (eV)	E_{gd} (eV) (direct)	E_{gi} (eV) (indirect)	E_u (eV)	
0	–	–	–	3.35	1.3	0.63	–
1	2	1.75	0.11	2.25	1.8	0.17	550
2.5	1.95	1.7	0.13	2.1	1.6	0.35	570
4	1.93	1.75	0.1	2.1	1.5	0.3	585
5	1.92	1.71	0.13	2.6	2	0.5	580
6	1.95	1.75	0.12	1.7	1.4	0.085	565
7.5	2.2	1.75	0.25	1.7	1.45	0.15	495
10	1.9	1.65	0.15	1.7	1.4	0.24	585
12.5	1.96	1.75	0.14	–	–	–	555
15	1.98	1.73	0.12	–	–	–	550

in colloidal (solution) and solid film form having different concentrations of CuI nanoparticles. It can be seen from these figures that the absorption peak position is affected with varying the concentration of CuI nanoparticles and shows red shift for solid films while the absorption peak for composite colloidal appears in narrow wavelength range (495–585 nm). In addition the absorption edge varies also with increasing the concentration of CuI nanoparticles in PVA polymer matrix. The optical band can be estimated from the following relationship [23]

$$(\alpha h\nu)^{1/n} = A(h\nu - E_g) \quad (2)$$

where A is constant; E_g is the optical band gap of the material and the exponent n depends on the type of transition, where it is equal to 1/2 for direct, allowed transition. The direct optical band gaps were obtained by the least square fitting, and the values of

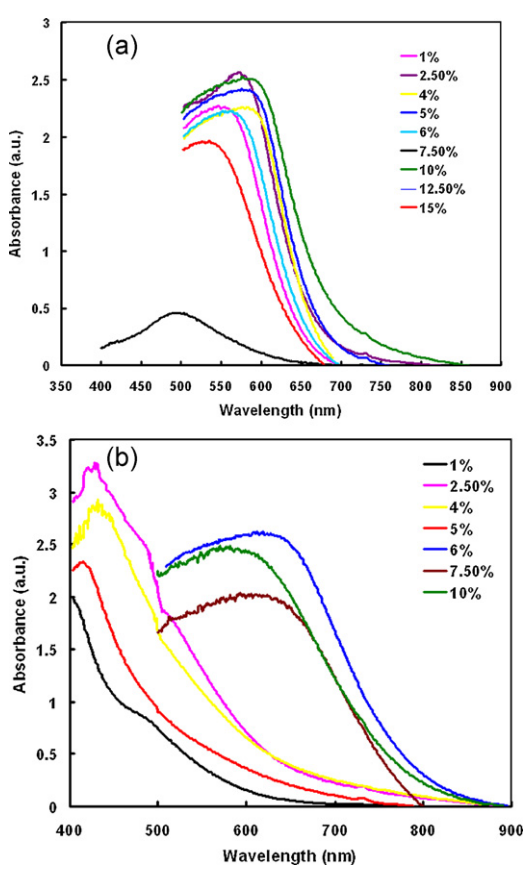

Fig. 3. Optical absorption spectra for (a) colloidal and (b) solid films of CuI/PVA polymer composites with different concentrations of CuI in colloidal form.

E_g were obtained for direct and indirect transitions for both colloidal and solid films and listed in Table 1. It is evident that the average value of E_g for PVA–CuI composite in colloidal form is equal to 1.73 and 1.97 eV for direct and indirect transitions, respectively, whereas the band gap lies in the range 1.7–2.25 eV for direct transitions and 1.4–1.8 eV for indirect transition. In general, direct band gap E_g decreases with increasing CuI concentration in the case of solid films (from 3.35 eV to 1.7 eV); this can be attributed to the salt complexation with the polymer matrix besides the expected nanoparticle aggregation. It is known that semiconductor nanoparticles have unique size-dependent chemical and physical properties. As the size of semiconductor particles decreases to the nanoscale, the band gap of the semiconductor increases, causing a blue shift in the UV–vis absorption spectra due to quantum confinement [24]. It is also clear that the values of E_g for both directly and indirectly allowed transitions in the case of polymer/CuI composites colloidal did not vary with the variation of CuI nanoparticle concentration, whereas they changed with varying the concentration of CuI due to the formation of aggregates in solid phase polymer composite. The increase in the absorption and decrease in the band gap may be due to a larger absorption increment associated with the charge transfer transition [25]. The absorption coefficient near the fundamental absorption edge is exponentially dependent on the incident photon energy and obeys the empirical Urbach relation [26]

$$\alpha = \alpha_o \exp\left(\frac{h\upsilon}{E_u}\right) \quad (3)$$

where E_u is the optical activation energy known as the Urbach energy which represents the band width of the tail of localized states in the band gap, and α_o is constant. The optical activation energy, E_u was determined using the least square fitting and listed in Table 1. The magnitudes of E_b obtained from conductivity data are larger than E_u values (see Tables 1 and 3). This is due to the fact that their nature is different. The activation energy corresponds to the energy required for conduction from one site to another, whereas the optical band gap corresponds to inter-band transition.

3.3. Electrochemical studies

The highest occupied molecular orbital (HOMO) and lowest unoccupied molecular orbital (LUMO) energy levels of polymer are important parameters in the design optoelectronic devices, and can be estimated from the onset oxidation (E^{ox}_{onset}) and reduction (E^{ox}_{onset}) potentials vs Ag/Ag$^+$. The HOMO and LUMO energy levels are estimated from the following equations [27]:

$$E_{HOMO} = -q(E^{ox}_{onset} + 4.7)\ \text{eV}$$
$$E_{LUMO} = -q(E^{red}_{onset} + 4.7)\ \text{eV} \quad (4)$$

Table 2
Oxidation and reduction onset potentials for the CuI/PVA composites. The values of HOMO, LUMO levels and electrochemical band gap are also included.

CuI concentration in composites	E^{ox}_{onset} (V)	E^{red}_{onset} (V)	E_{HOMO} (eV)	E_{LUMO} (eV)	E^{elec}_{g} (eV)
1%	0.75	−1.55	−5.45	−2.95	2.50
2.5%	0.50	−1.66	−5.20	−3.04	2.16
6%	0.4	−1.44	−5.10	−3.26	1.84
10%	0.4	−1.4	−5.10	−3.3	1.80

Q11 The values of E^{ox}_{onset}, E^{red}_{onset}, HOMO and LUMO for the different Q12 CuI–PVA composites are summarized in Table 2. It can be seen that HOMO level (ionization potential) decreases (shift toward the vacuum level) and the LUMO level (electron affinity) increases (shifts away from the vacuum level) as the concentration of the CuI increases, leading to a decrease in the electrochemical band gap (difference between the HOMO and LUMO energy level) that agrees with the trend observed in the optical band measured from the absorption spectra of composites in thin film form.

3.4. AC spectroscopy

Fig. 4 illustrates the impedance plot of the imaginary part, Z'', against the real part, Z', for CuI-polymer nanocomposites at room temperature as representative diagram. The impedance plot, in general, shows an arc (semicircle), its center below the Z' axis, the intersection with Z' axis, represents the bulk resistance, R_b [28]. It is observed that the circle diameter varies with increasing CuI concentration. The values of bulk conductivity of the CuI-polymer composites were obtained, using $\sigma_b = dR_b/A$ (where d is the film thickness and A is its effective area) for different concentrations of CuI in the polymer composites. Fig. 5 illustrates the bulk conductivity obtained against concentrations of CuI (=0–15 wt%). It can be seen from this figure that bulk conductivity increases as the increase in the CuI concentration up to 4% then starts to decrease as the concentration of CuI further increases. Fig. 6 illustrates temperature dependence of bulk conductivity for different concentrations, C(=0–15 wt%); they illustrate clearly that the conductivity is thermally activated with increasing temperature and follows the Arrhenius relation,

$$\sigma_b T = \sigma_{bo} \exp\left(-\frac{E_b}{kT}\right) \quad (5)$$

where E_b is the bulk conductivity activation energy and σ_{bo} is the Q13 bulk conductivity at $T = \infty$. The results illustrate the two regions' characterizing conduction at relatively low and high temperature respectively. The values of E_b are obtained by least square fitting for the two regions and listed in Table 3, and lie in the range 0.27–1.02 and 0.29–0.64 eV respectively. The transition between the two regions refers to the composite T_g. It is clearly observed that E_b varies irregularly with CuI concentration which can be attributed to the composite structure and salt complexation with polymer matrix.

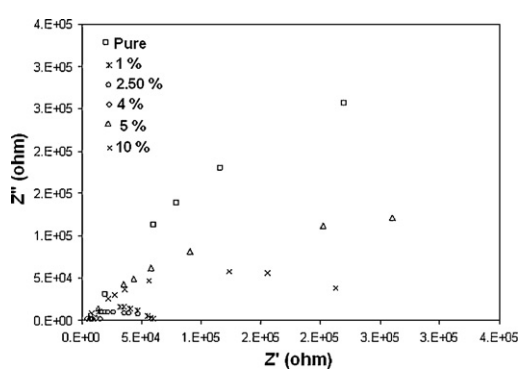

Fig. 4. Impedance plots (Cole–Cole plots) for CuI/PVA polymer composites with different concentration of CuI.

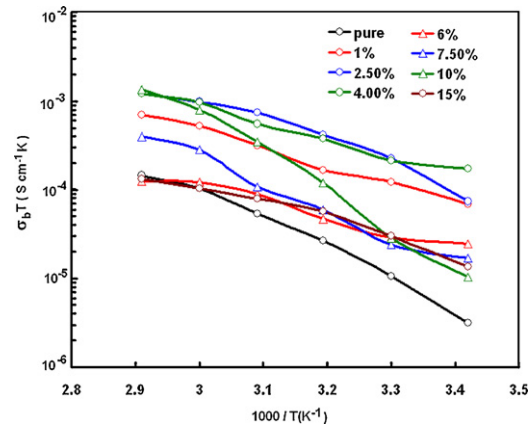

Fig. 5. Temperature dependent bulk conductivity σ_b for all prepared CuI/PVA polymer composites for different concentration of CuI.

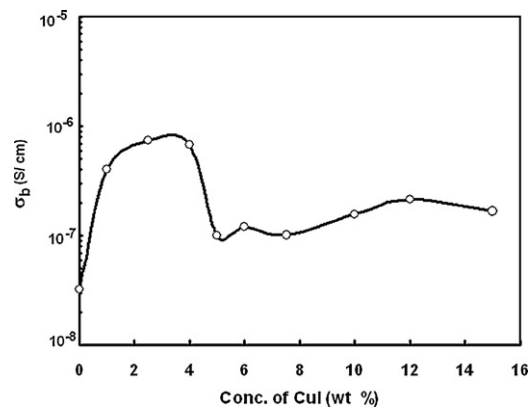

Fig. 6. Variation of bulk conductivity with the concentration of CuI for PVA/CuI polymer composites at room temperature.

3.5. Current–voltage characteristics in dark and under illumination

We have investigated the current–voltage (J–V) characteristics of CuI–PVA composite using the device structure ITO/PEDOT:PSS/CuI–PVA/Al, in dark which are shown in Fig. 7. The J–V characteristics of the devices in the dark show a rectification effect when positive potential is applied to the ITO/PEDOT:PSS

Table 3
Obtained bulk conductivity activation energy and particle sizes for PVA/CuI solid layers.

Conc. of CuI	E_a (eV)		Particle size
	Region I	Region II	
Pure	0.795073	0.368756	–
1%	0.397265	–	–
2.5%	0.749063	0.293488	31
4%	0.332639	–	–
5%	1.018555	0.563066	25.6
6%	0.269289	–	–
7.5%	0.55171	–	–
10%	0.92514	0.642014	42
12.5%	0.593657	–	46.7
15%	0.311364	–	46.3

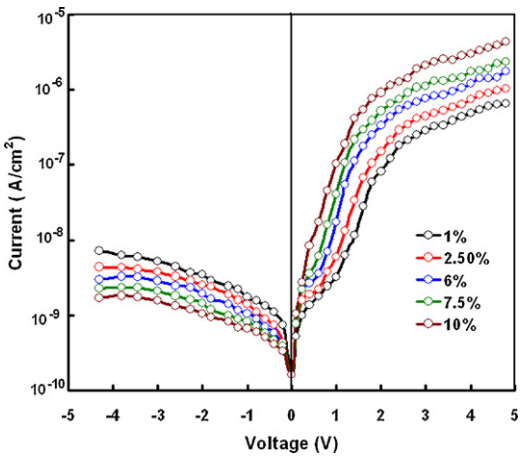

Fig. 7. Current–voltage (J–V) characteristics of the ITO/PEDOT:PSS/CuI–PVA composite/Al with different concentration of CuI in composite.

electrode with respect to Al electrode. Since the HOMO level of CuI–PVA composites (−4.9 to 5.35 eV) is very close to the HOMO level of PEDOT:PSS, this electrode behaves as Ohmic contact for hole injection from the ITO/PEDOT:PSS electrode into the HOMO level of the composite. However, the LUMO level of all composites is very far from the work function of the Al electrode (−4.2 eV) and forms a Schottky barrier for the electron injection from the Al into the LUMO level of composite. Therefore the rectification is due to the formation of the Schottky barrier at the Al/PVA–CuI interface.

The charge carrier mobility of an organic semiconductor can be extracted from the J–V characteristics of a device in which both the electrodes form Ohmic contact with the organic semiconductor film. We have measured the J–V characteristics of the device having ITO/PEDOT:PSS/CuI–PVA/Au structure to estimate the hole mobilities in different PVA–CuI composites. Fig. 8 shows the J–V characteristics of the devices based on different CuI–PVA composites, in dark. It can be seen from these plots that the current increases continuously with the increase in the concentration of CuI particles embedded in PVA. This can be explained on the basis of formation of charge transfer complexes within the PVA matrix, which facilitates the delocalization of conduction electrons resulting in increase in the current [29].

The J–V characteristics show a space charge current limited with trap free limit in higher voltage region above 1.0 V. This SCLC

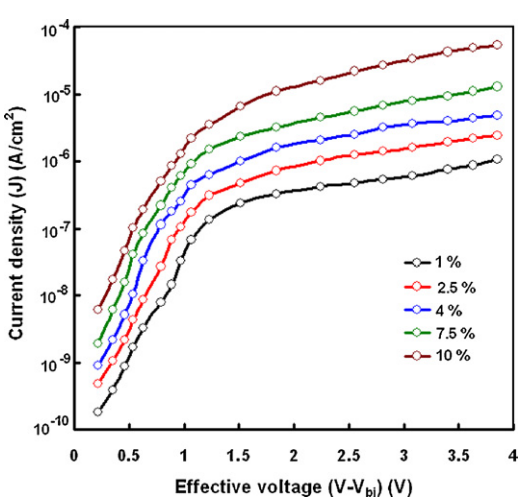

Fig. 8. Current–voltage (J–V) of the ITO/PEDOT:PSS/CuI–PVA/Au device, with different concentration of CuI in composite to estimate the hole mobility.

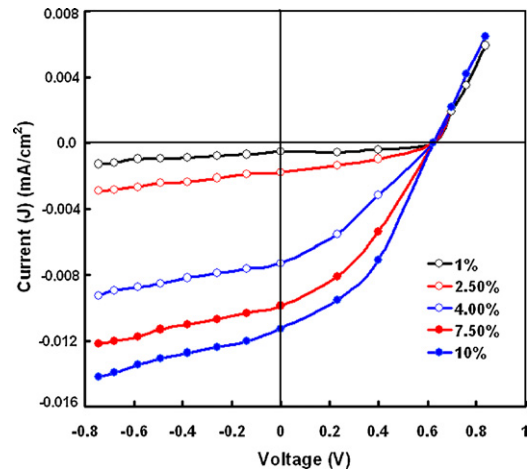

Fig. 9. Current–voltage characteristics of the ITO/PEDOT:PSS/CuI–PVA/Al devices, with different concentration of CuI in the composites, under illumination intensity of 100 mW/cm^2.

behavior can be characterized by the Mott–Gurney law, described as [30]

$$J = \left(\frac{9}{8}\right)\varepsilon\mu\left(\frac{V^2}{d^3}\right)$$

where ε is the static dielectric constant of the organic composite layer, μ is the hole mobility, d is the thickness of the layer and V is the effective voltage, which is corrected for built-in voltage. The hole mobility in these composite layers has been estimated through the fitting of J–V characteristics in higher voltage region with equation. The values of the hole mobility are complied in Table 4. It was found that the hole mobilities increase with the increase in the concentration of the CuI nanoparticles in the composite. This is in agreement with the trend observed in the bulk conductivity of the composites as described earlier.

The J–V characteristics of the ITO/PEDOT:PSS/CuI–PVA composites/Al devices under illumination intensity are shown in Fig. 9 and photovoltaic parameters i.e. short circuit current (J_{sc}), open circuit voltage (V_{oc}), fill factor (FF) and power conversion efficiency are complied in Table 4. The PCE value of the device increases as the concentration of the CuI in the composite is increased. This is mainly due to the increase in the J_{sc}, as the concentration of CuI is increased. As we have discussed above, the hole mobility has been improved with the increase of the CuI concentration, we conclude that the increase in the J_{sc} is mainly due to the improvement in the hole mobility, as the crystalline nature of the composite has been increased [31]. In spite of the broader absorption in the longer wavelength region and shift in the absorption edge toward the longer wavelength region as the incorporation of CuI in the PVA matrix, the PCE of the devices is very small. This feature is attributed to the fact that all the excitons generated in the composite layer, after the absorption of light, are not dissociated into free charge carriers, because of the short exciton diffusion length in the organic layer. Since the built-in potential present at the interface at the Al/CuI–PVA interface in the device is responsible for the exciton dissociation into free carrier, only the photogenerated excitons are able to reach this interface, and contribute to the photocurrent. The excitons generated faraway from this interface are decayed during their diffusion toward this interface and do not contribute to the photocurrent and thus leading to low PCE. However, we expect that when these blends used as electron donor with fullerene derivatives as electron acceptor may give higher PCE. This work is under progress and will be reported later on.

Table 4
Photovoltaic parameters of the device with different concentration of CuI in the composite. The hole mobility is also given.

Concentration of CuI in composite (wt%)	J_{sc} (mA/cm^2)	V_{oc} (V)	FF	PCE (%) ($\times 10^{-3}$)	Mobility (cm^2/V s)
1%	0.00055	0.62	0.23	0.0078	3.4×10^{-7}
2.5%	0.0018	0.64	0.28	0.031	8.8×10^{-7}
4%	0.0078	0.63	0.32	1.6	2.5×10^{-6}
7.5%	0.0098	0.63	0.35	2.1	6.7×10^{-6}
10%	0.011	0.63	0.38	2.6	8.9×10^{-6}

4. Conclusions

We have prepared CuI/PVA nanopolymer composites with different concentration of CuI up to 15% by wt. The characterization using XRD demonstrated that the nano-CuI particles (26–46 nm) grew in PVA polymer matrix whereas the degree of crystallinity of PVA was reduced with increasing CuI. The activation energy estimated from the temperature variation of bulk conductivity fluctuates between 0.27 and 1.02 eV. The study of optical absorption in UV–visible range illustrated significant decreases of the optical energy gap with increasing CuI nanoparticles in PVA polymer matrix solid films whereas it is nearly unchanged in the case of colloidal phase (the average value of E_{gd} and $E_{g\,ind}$ is equal to 173 and 1.97 eV respectively). The electrochemical band gap estimated from the cyclic voltammetry agrees well with the trend observed with the optical band gap. The J–V characteristics of the devices, having structure ITO/PEDOT:PSS/CuI–PVA composites/Al, in dark, show rectification effect which is due to the formation of Schottky barrier and Ohmic contact with Al and ITO/PEDOT:PSS electrodes, respectively. This can be easily understood in terms of the HOMO and LUMO energy levels of composites with respect to the work functions of both electrodes. The hole mobility in the composite Q14 blend increases with the concentration of CuI particles in composites which is attributed to the increased crystalline nature of the composite. The PCE of the devices using the composites without the electron acceptor is low but it can be increased when these composites are used as electron donors along with the fullerene derivatives as electron acceptor in bulk heterojunction organic solar cells. The work is under progress and will be reported later on.

Acknowledgment

This project was supported financially by the Science and Technology Development Fund (STDF), Egypt, Grant No. 1360.

References

[1] (a) D.Y. Godovsky, Device applications of polymer nanocomposites, Adv. Polym. Sci. 153 (2000) 163–205;
(b) F.C. Krebs, T.D. Nelson, J. Fyenbo, M. Wadstrom, M.S. Pedersen, Manufacture, integration, demonstration of polymer solar cells in a lamp for "Lighting Africa" initiative, Energy Environ. Sci. 3 (2010) 512–525;
(c) B.C. Thompson, J.M.J. Frechet, Polymer–fullerene composite solar cells, Angew. Chem. Int. Ed. 47 (2008) 58–77.
[2] (a) S. Genes, H. Neugebauer, N.S. Sariciftci, Conjugated polymer based organic solar cells, Chem. Rev. 107 (2007) 1324–1338;
(b) J.A. Mikroyannidis, A.N. Kabanakis, S.S. Sharma, G.D. Sharma, Low band gap phenylene vinylene and fluorenevinylene small molecules containing triphenylamine segments: synthesis and application in bulk heterojunction solar cells, Org. Electron. 12 (2011) 774–784.
[3] (a) A.C. Mayer, S.R. Scully, B.E. Hardin, M.W. Rowell, M.D. McGehee, Polymer based solar cells, Mater. Today 10 (2007) 28–33;
(b) R. Po, M. Maggini, N. Camaioni, Polymer solar cells: recent approaches and achievements, J. Phys. Chem. C 114 (2010) 695–706;
(c) J.A. Mikroyannidis, D.V. Tsagkournosa, P. Balraju, G.D. Sharma, Synthesis and photovoltaic properties of an alternating phenylenevinylene copolymer with substituted triphenylamine units along with backbone for bulk heterojunction and dye sensitized solar cells, J. Power Sources 196 (2011) 2364–2372.
[4] (a) F.C. Krebs, T. Tromholt, M. Jorgensen, Upscaling of polymer solar cell fabrication using roll to roll processing, Nanoscale 2 (2010) 873–886;
(b) J.A. Mikroyannidis, D.V. Tsakournos, S.S. Sharma, Y.K. Vijay, G.D. Sharma, Conjugated small molecules with broad absorption containing pyridine and pyran units: synthesis and application for bulk heterojunction solar cells, Org. Electron. 11 (2010) 2045–2054.
[5] (a) M. Helgesen, R. Sondergaard, F.C. Krebs, Advance materials and processes for polymer solar cell devices, J. Mater. Chem. 20 (2010) 36–60;
(b) J.A. Mikroyannidis, D.V. Tsagkournos, S.S. Sharma, Anil Kumar, Y.K. Vijay, G.D. Sharma, Efficient bulk heterojunction solar cells based on low band gap bisazodyes containing anthracene and/or pyrrole units, Sol. Energy Mater. Sol. Cells 94 (2010) 2317–2318.
[6] C. Kanimozhi, P. Balraju, G.D. Sharma, S. Patil, Synthesis of diketopyrrolopyrrole containing copolymers: a study of their optical and photovoltaic properties, J. Phys. Chem. B 114 (2010) 3095–4003.
[7] E. Sheha, H. Khoder, T.S. Shanap, M.G. El-Shaarawy, M.K. El Mansy, Structure, dielectric and optical properties of p-type (PVA/CuI) Q15 nano-composite polymer electrolyte for photovoltaic cells, Optik, http://dx.doi.org/10.1016/j.ijleo.2011.06.066.
[8] E. Sheha, M.K. El-Mans, A high voltage magnesium battery based on H_2SO_4-doped $(PVA)_{0.7}(NaBr)_{0.3}$ solid polymer electrolyte, J. Power Sources 185 (2008) 1509–1513.
[9] (a) L. Huo, J. Hou, S. Zhang, H.Y. Chen, Y. Yang, A poly [1,2-b:4,5-b'] dithiophene derivatives with deep HOMO level and its application in high performance polymer solar cells, Angew. Chem. Int. Ed. 49 (2010) 1500–1503;
(b) Y. Zhou, A. Naiari, P. Berrouard, S. Beaupre, B.R. Aich, Y. Tao, M. Leclerc, A thieno [3,4-c] pyrrole-4,6-dione based copolymer for efficient solar cells, J. Am. Chem. Soc. 132 (2010) 5330–5331;
(c) H.Y. Chen, J. Hou, S. Zhang, Y. Liang, G. Yang, L. Yu, Y. Wu, G. Li, Polymer solar cells with enhanced open circuit voltage and efficiency, Nat. Photon. 3 (2009) 649–653;
(d) S.H. Park, A. Roy, S. Beaupre, S. Cho, N. Coates, J.S. Moon, D. Moses, M. Leclerc, K. Lee, A.J. Heeger, Bulk heterojunction solar cells with internal quantum efficiency approaching 100%, Nat. Photon. 3 (2009) 297–302;
(e) Y. Linag, Z. Xu, J. Xia, S.T. Tsai, Y. Wu, G. Li, C. Ray, L. Yu, For the bright future-bulk heterojunction polymer solar cells with power conversion efficiency of 7.4%, Adv. Mater. 22 (2010) E135–E138;
(f) J.A. Mikroyannidis, A.N. Kabanakis, S.S. Sharma, G.D. Sharma, A simple and effective modification of PCBM for use as an electron acceptor in efficient bulk heterojunction solar cells, Adv. Funct. Mater. 21 (2011) 746–755.
[10] (a) www:solarmer.com;
(b) www:konarka.com.
[11] (a) P.W.M. Blom, H.F.M. Schoo, M. Matters, Electrical characterization of electroluminescent polymer/nanoparticle composites, Appl. Phys. Lett. 73 (1998) 3914;
(b) A. Kiesow, J.E. Morris, C. Radehaus, A. Heilmann, Switching behavior of plasama polymer films containing silver nanoparticle, J. Appl. Phys. 94 (2003) 6988–6991.
[12] A. Gautam, S. Ram, Preparation and thermomechainical properties of Ag-PVA nano-composite films, Mater. Chem. Phys. 119 (2010) 266–271.
[13] K.A. Abdelkader, Z. Anwar, Sepctroscopic studies of poly vinyl alcohol, J. Appl. Polym. Sci. 2 (2006) 1146–1151.
[14] K. Tennakone, G.R.R.A. Kumara, I.R.M. Kottegoda, V.P.S. Perera, G.M.L.P. Aponsu, K.G.U. Wijayantha, Deposition of thin film conducting film of CuI on glass, Sol. Q16 Energy Mater. Sol. Cells 55 (1998) 283.
[15] G.R.R.A. Kumara, A. Konno, G.K.R. Senadeera, P.V.V. Jayaweere, D.B.R.A. De Silva, T. Tennakone, Dye sensitized solar cells with hole collector p-CuSCN deposited from a solution in propyl sulphide, Sol. Energy Mater. Sol. Cells 69 (2001) 195–199.
[16] K. Tonooka, K. Shimokawa, O. Nishimura, Properties of copper–aluminum oxide films prepared by solution methods, Thin Solid Films 411 (2002) 129–133.
[17] S.L. Dherea, S.S. Latthea, C. Kappenstein, S.K. Mukherjee, A. Venkateswara Rao, Comparative studies on p-type CuI grown on glass and copper substrate by SILAR method, Appl. Surf. Sci. 256 (12) (2010) 3967–3971.
[18] P.V. Kamat, Interfacial charge transfer processes in colloidal semiconductor systems, Prog. React. Kinet. 19 (1994) 277–316.
[19] C.B. Murray, C.R. Kagan, M.G. Bawendi, Self organization of CdSe nanocrystallites into three dimensional quantum dot super lattices, Science 270 (1995) 1335–1338.
[20] B.Z. Tong, Y. Geng, J.W.Y. Lam, B. Li, X. Jing, X. Wang, F. Wang, A.B. Pakhomov, X.X. Zhang, Processible nanostructured materials with electrical conductivity and magnetic susceptibility: preparation and properties of maghemite/polyaniline nanocomposites, Chem. Mater. 11 (1999) 1581–1589.
[21] R.M. Hodge, G.H. Edward, G.P. Simon, Water absorption and states of water in semi-crystalline poly (vinyl alcohol) films, Polymer 37 (1996) 1371–1376.
[22] B. Pejova, I. Grozdanov, Three dimensional confinement effects in semiconducting zinc selenide quantum dots deposited in thin film form, Mater. Chem. Phys. 90 (2005) 35–46.

[23] (a) Y. Aydogdu, F. Yakuphanoglu, A. Aydogdu, E. Tas, A. Cukuraval, Electrical and optical properties of newly synthesized glyoxime complexes, Solid State Sci. 4 (2002) 879–883;
(b) E.A. Davis, N.F. Mott, Conduction in non-crystalline systems V, conductivity, optical absorption and photoconductivity in amorphous semiconductors, Philos. Mag. 22 (1970) 903–922.
[24] H. Wang, P. Fang, Z. Chen, S. Wang, Synthesis and characterization of CdS/PVA nanocomposite films, Appl. Surf. Sci. 253 (2007) 8495–8499.
[25] E.S. Mora, E.G. Barojas, E.R. Rojas, R.S. Gonzalez, Morphological, optical and photocatalytic properties of TiO_2–Fe_2O_3 multi-layers, Sol. Energy Mater. Sol. Cells 91 (2007) 1412–1415.
Q17 [26] F. Urbach, The long wavelength edge of photographic sensitivity of the electron absorption of solids, Phys. Rev. 92 (1953) 1324.
[27] (a) Y. Li, Y. Cao, J. Gao, D. Wang, G. Yu, A.J. Heeger, Electrochemical properties of luminescent polymers and polymer light emitting electrochemical cells, Synth. Met. 99 (1999) 243–248;
(b) Q.J. Sun, H.Q. Wang, C.H. Yang, Y.F. Li, Synthesis and electroluminescence of novel copolymers containing crown ether spacers, J. Mater. Chem. 13 (2003) 800–806.
[28] N.M. Shash, F.E. Salman, A.Z. Mohamed, M.G. El-Sharawy, R.M. Bayomi, M.K. El-Mansy, Effect of verification suppression on structure morphology, conductivity, and dielectric properties of vanadium phosphate glasses, J. Phys. Chem. Solids 65 (2004) 881–889.
[29] C.U. Devi, A.K. Sharma, V.V.R.N. Rao, Electrical and optical properties of pure and silver nitrate doped poly vinyl alcohol films, Mater. Lett. 56 (2002) 167–174.
[30] (a) M.A. Lampert, P. Mark, Current Injection in Solids, Academic Press, New York, 1970;
(b) V.D. Mihaitetchi, H. Xie, B. de Boer, L.J.A. Koster, P.W.M. Blom, Charge transport and photocurrent generation in poly (3-hexylthiophene): methenofullerene bulk heterojunction solar cells, Adv. Funct. Mater. 16 (2006) 699–708;
(c) Y. Zhao, Z. Xie, Y. Qu, Y. Geng, L. Wang, Solvent vapor treatement indued perfromance enhencement of poly (3-hexylthiophene): methenofullerene bulk heterojunction solar cells, Appl. Phys. Lett. 90 (2007), 043504/1-3.
[31] (a) J.A. Mikroyannidis, A.N. Kabanakis, P. Suresh, G.D. Sharma, Efficient bulk heterojunction solar cells based on a broadly absorbing phenylenevinylene copolymer containing thiophene and pyrrole rings, J. Phys. Chem. C 115 (2011) 7056–7066;
(b) A. Tamayo, T. Kent, M. Tantitiwat, M.A. Dante, J. Rogers, T.Q. Nguyen, Influence of alkyl substituents and thermal annealing on the film morphology and performance of solution processed diketopyrrolopyrrole based bulk heterojunction solar cells, Energy Environ. Sci. 2 (2009) 1180–1186.

Please cite this article in press as: M.K. El-Mansy, et al., Characterization of PVA/CuI polymer composites as electron donor for photovoltaic application, Optik - Int. J. Light Electron Opt. (2012), http://dx.doi.org/10.1016/j.ijleo.2012.05.009